Circulation: Arrhythmia and Electrophysiology

REVIEW

Differentiating Right- and Left-Sided Outflow Tract Ventricular Arrhythmias

Classical ECG Signatures and Prediction Algorithms

ABSTRACT: Idiopathic ventricular arrhythmias commonly originate from the right ventricular and left ventricular outflow tracts (OTs). Advances in real-time imaging have refined our understanding of the intimate anatomic structures implicated in the genesis of OT arrhythmias, making catheter ablation for arrhythmias beyond the right ventricular OT a feasible option for cure—indeed ablation is now a class I indication in recent guidelines. The surface 12-lead ECG is routinely used to localize the anatomic site of origin before catheter ablation. However, the intimate and complex anatomy of the OT limits predictive value ECG criteria alone for localization for these arrhythmias. Multiple ECG algorithms have been developed to assist preprocedural localization, and hence predict safety and efficacy for catheter ablation of OT ventricular arrhythmias. This review will summarize all of the published 12-lead ECG algorithms used to guide localization of OT ventricular arrhythmias.

Robert D. Anderson, MBBS
Saurabh Kumar, BSc(Med)/MBBS, PhD
Ramanathan Parameswaran, MBBS
Geoffrey Wong, MBBS
Aleksandr Voskoboinik, MBBS
Hariharan Sugumar, MBBS
Troy Watts, BSc
Paul B. Sparks, MBBS, PhD
Joseph B. Morton, MBBS, PhD
Alex McLellan, MBBS, PhD
Peter M. Kistler, MBBS, PhD
Jonathan Kalman, MBBS, PhD
Geoffrey Lee, MBChB, PhD

Outflow tract ventricular arrhythmias (OTVAs) are the most common type of idiopathic VA. It typically presents in young patients—and has a notably increasing incidence.[1] It is classically a benign, focal arrhythmia but patients can be highly symptomatic and refractory to medical therapy. Moreover, frequent ectopy can progress to a premature ventricular complex (PVC)–induced cardiomyopathy. For both indications, catheter ablation (CA) can be considered. CA has a low procedural complication risk (<1%) that is outweighed generally, by a high success rate with long-term probability of cure. Before CA, it is imperative to have an appreciation of the OTVA origin. Distinguishing between right or left OT site of origin (SOO) preprocedurally is useful in terms of guiding access for the ablation, counseling patients on specific risks and may even involve referral to a specialist unit if localized to a high-risk or difficult position.

The surface ECG is a simple noninvasive tool and is particularly conducive to localize the SOO of ectopic foci in patients with structurally normal hearts, but the close anatomic proximity of the OTs and the complex overlay of the anterior and leftward directed right ventricular OT (RVOT) with the posterior and rightward directed left ventricular OT (LVOT) makes clear separation and the application of morphological characteristics at each site challenging. This has led to the creation of a number of algorithms to refine the predictive accuracy of ECG localization including the development of new ECG configurations. We reviewed published algorithms to assess their clinical utility and applicability different types of OTVA.

Key Words: algorithms ■ cardiac arrhythmia ■ catheter ablation ■ electrocardiography

© 2019 American Heart Association, Inc.

https://www.ahajournals.org/journal/circep

Downloaded from http://ahajournals.org by on May 28, 2022

CLASSICAL ECG SIGNATURES OF RVOT SITES

The majority (70%–80%) of OTVAs originates from the RVOT and is the most common SOO.[2] The RVOT is tubular structure located anterior and leftward relative to the LVOT (Figure 1). It is bounded cranially by the pulmonary valve (orientated horizontally and 1–2 cm superior to the aortic valve) and caudally by the RV inflow/top of tricuspid valve (orientated vertically). The RVOT is divided into rightward (referred to as free wall), anterior, leftward, and posterior (referred to as septal) parts.[4] The posterior RVOT is directly anterior to the LVOT and anterior interventricular septum, separated by the ventriculo-infundibular fold that extends between the septomarginal trabeculation and pulmonary valve.[5] It is important to highlight that the more distal posterior RVOT is adjacent to the sinus of Valsalva and aortic leaflets: right coronary aortic sinus (RCAS) and part of the left coronary aortic sinus (LCAS). The anteroseptum is in close proximity to the LV epicardium and summit (Figure 1). The following summarizes all published ECG features from specific RVOT sites (Figure 2; Table 1).

RVOT: Septal and Free-Wall Sites

Early pacemapping studies established the typical morphological features of RVOT foci.[6,7] In their series of patients with structurally normal hearts, Jadonath et al,[6] divided the RVOT in 11 patients into 9 distinct sites. In all locations, a QS was seen in aVR and a monophasic R wave in the inferior leads. Lead I discriminated posterior and anterior sites: a Q wave pointed to an anterior site (qR, Qs, and Qr), whereas pacing posteriorly produced an R wave (monophasic R, Rs). Although less discriminatory than lead I, aVL was used to differentiate anterior and posterior sites. Anterior sites always produced a QS in aVL, whereas an R wave was always present in posterior sites (qR, rS, and rSr).

Other morphological features were described by Dixit et al,[12] where pace maps were generated from different locations in the RVOT in 14 patients. Septal RVOT sites showed taller R-wave amplitude in the inferior leads, were narrower, had an earlier transition ($<V_4$) and lacked notching (monophasic) compared to free-wall sites. Notching is potentially explained by sequential (not simultaneous) RV and LV activation when the free wall is paced. Similar morphological characteristics were described by Joshi et al.[8] A QRS duration ≥140 ms with R-wave notching in ≥2 inferior leads has a sensitivity of 74% and specificity of 93% to predict a free-wall RVOT site.[8] A negative or isoelectric QRS in lead I positioned the site anterior and an isoelectric or positive QRS in aVL placed the site caudal (>2 cm from the pulmonary valve) with high sensitivity and specificity (96% and 86%, respectively).

Pulmonary Valvular Sinuses

A small proportion of OTVAs (≈4%) originate from above (>10 mm) the pulmonary trunk or pulmonary leaflets and can be mapped with a reversed U-shape configuration of the ablation catheter to allow mapping on top of the valve leaflets.[9–11] Histologically, the pulmonic valve leaflets have thin sleeves of myocardial musculature extensions from the RVOT admixed with fibrous and fatty tissue (containing ganglionated plexuses influenced by the autonomic nervous system) contributing to this sites arrhythmogenesis.[28]

The 3 pulmonary valvular sinuses are located posteriorly (left cusp), anterosuperior septal (anterior cusp), and anterosuperior rightward (right cusp). The pulmonary valvular sinuses are not at the same level: left cusp is the lowest with the anterior cusp and right cusp being more superior. Compared to the anterior cusp and left cusp, a right cusp origin classically has larger R wave in lead I, notching in the inferior leads and a smaller aVL/aVR ratio (of the Q-wave amplitude)[29] (Figure 2; Table 2). It is important to recognize that the left cusp of the pulmonary valve is intimately related to the left main coronary artery and the anterior horn of the RV can be in close proximity to the mid-left anterior descending (Figure 3B and 3C).[30,31] Pulmonary artery VAs typically shows tall R-wave amplitudes inferiorly and greater aVL/aVR ratio[32] due to the extreme leftward orientation of the pulmonary artery compared to the other relevant structures.

CLASSICAL ECG SIGNATURES OF LVOT SITES

Less commonly (15%–25%), idiopathic ventricular tachycardia (VT) originates from the LVOT.[33] Anatomically, it occupies the central location in the heart and is bounded by the aortic root, aortomitral continuity (AMC), the superior basal septum and LV summit. The left and right aortic sinuses sit adjacent to the left and right atrial appendages, respectively. The nomenclature of the OTVA origins from the aortic valvular sinuses must be clarified. Although ablation sites are commonly referred to as coronary cusps, this term is misleading as myocardial arrhythmogenic tissue arises from the bases of the aortic sinuses or the interleaflet commissures.[28] Distinguishing these sites is clinically relevant as aortic sinus OTVA are optimally approached transaortically, typically wedged in tissue crescents at the base of the aortic sinuses. OTVA originating from interleaflet commissures may be better approached from below the leaflets to optimize proximity to the arrhythmogenic source and catheter stability. The posterior portion of the LVOT contains fibrous tissue and a septal region containing both fibrous and musculature tissue (Figure 1). The close anatomic relationship of the RVOT

Downloaded from http://ahajournals.org by on May 28, 2022

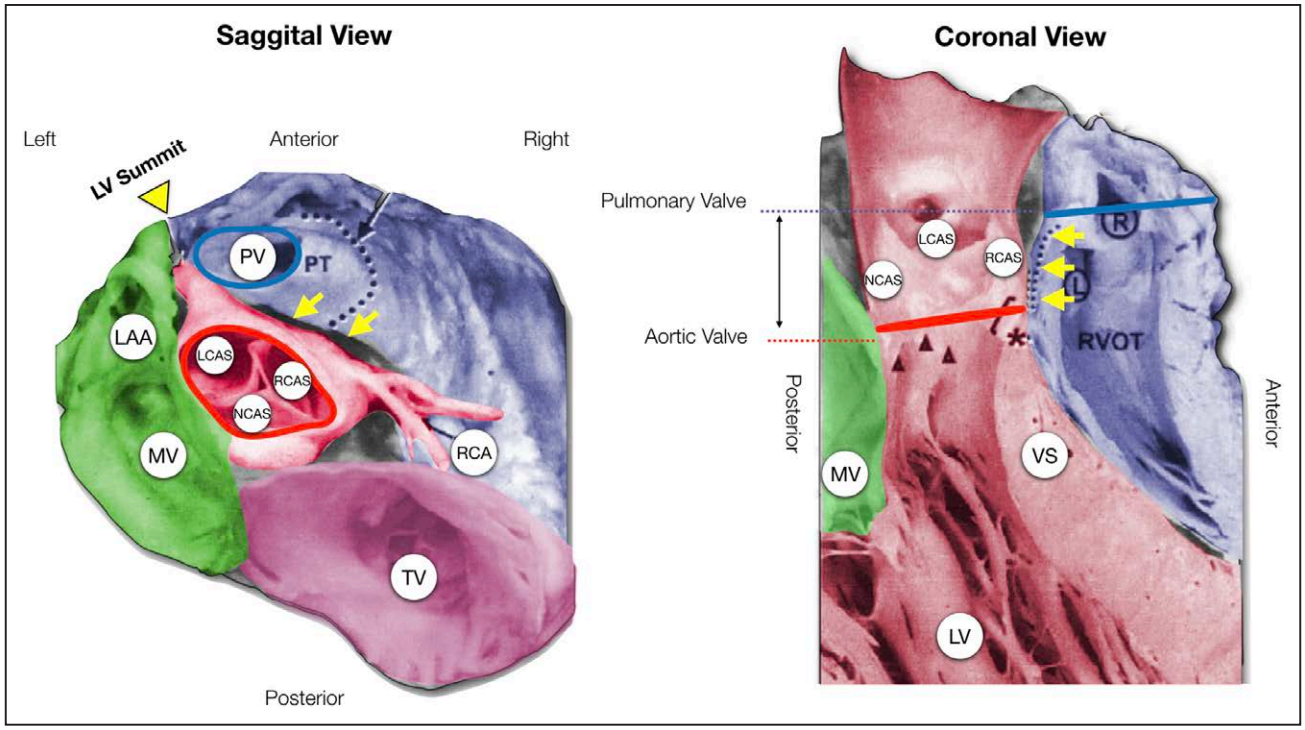

Figure 1. Illustration of typical sites of outflow tract ventricular arrhythmia (OTVA) sites using an anatomic model.
The left-sided image shows a sagittal section viewed posteriorly highlighting the relationship of the aortic (red circle) and pulmonary valves (PVs; blue circle). The right coronary aortic sinus (RCAS) and left coronary aortic sinus (LCAS) are most anterior, adjacent to the pulmonary infundibulum (yellow arrows) and the noncoronary aortic sinus (NCAS) is posterior. The dotted line represents the ventriculo-arterial junction dividing the pulmonary trunk and right ventricular (RV) muscle. The right-sided image shows the coronal image of the OT to highlight that the posterior septal right ventricular OT (RVOT) is adjacent to the left ventricular OT (LVOT), separated by the ventriculo-infundibular fold (yellow arrows). The PV (blue circle) is positioned 1 to 2 cm superior to the aortic valve (red circle). LAA indicates left atrial appendage; MV, mitral valve; PT, pulmonary trunk; RCA, right coronary artery; TV, tricuspid valve; and VS, ventricular septum. Adapted from Ouyang et al[3] with permission. Copyright © 2002, Elsevier.

Downloaded from http://ahajournals.org by on May 28, 2022

and LVOT can easily be appreciated on transesophageal and transthoracic echocardiography (Figure 3A). The following summarizes all the published ECG features from specific LV sites of origin (Figure 2; Tables 1 and 2).

Aortic Valvular Sinuses and Interleaflet Commissures

Foci from the aortic sinuses are reported to have a longer R-wave duration and earlier R/S transition in the precordial leads[3] than adjacent RVOT sites. The change in vector is proposed to be due to the posterior location of the aortic root, increasing the distance (and time) for the signal to reach V_1 or V_2.

RCAS

As the RCAS is positioned posterior to the septal RVOT, similar morphologies can be seen.[3] Pacing this site will produce a left bundle branch block (LBBB) pattern with a rS in V_1 and V_2 (small broad R wave) and transition in V_3.[17] Lead I can also be used to discriminate RCAS origins as its rightward annular position produces a more positive vector in this lead compared to the LCAS.[19,23]

LCAS

The more posterior LCAS produces an early R/S transition in V_1/V_2.[22] The R waves in V_1 and V_2 are characteristically tall and broad and the basis behind Ouyang's finding of a R wave >50% of the QRS duration combined with a R/S ratio of >30% was predictive of an LCAS origin.[3] The characteristic multiphasic M or W pattern in V_1 unique to this site has been explained by early transeptal activation from the LCAS.[17,18]

RCAS/LCAS

The seminal description of an arrhythmogenic source in the LCAS/RCAS commissure described a reproducible qrS pattern in V_1 through V_3 when pacing this site (n=5 patients).[16] Subsequently, Bala et al[15] identified a QS in V_1 (with notching in the downward deflection) and precordial transition in V_3 was seen in 15 of the 19 (79%) patients with an RCAS/LCAS focus and confirmed with electroanatomic mapping and intracardiac echocardiography.

Noncoronary Aortic Sinus

VAs are rarely seen at this site due to the proximity to the atrium and lack of myocardial sleeves.[3]

AMC and Anterolateral Mitral Annulus

Although once thought of consisting of fibrous tissue (wedged between the aortic and mitral valve annuli), the AMC region is a source of idiopathic VTs[20] due to the

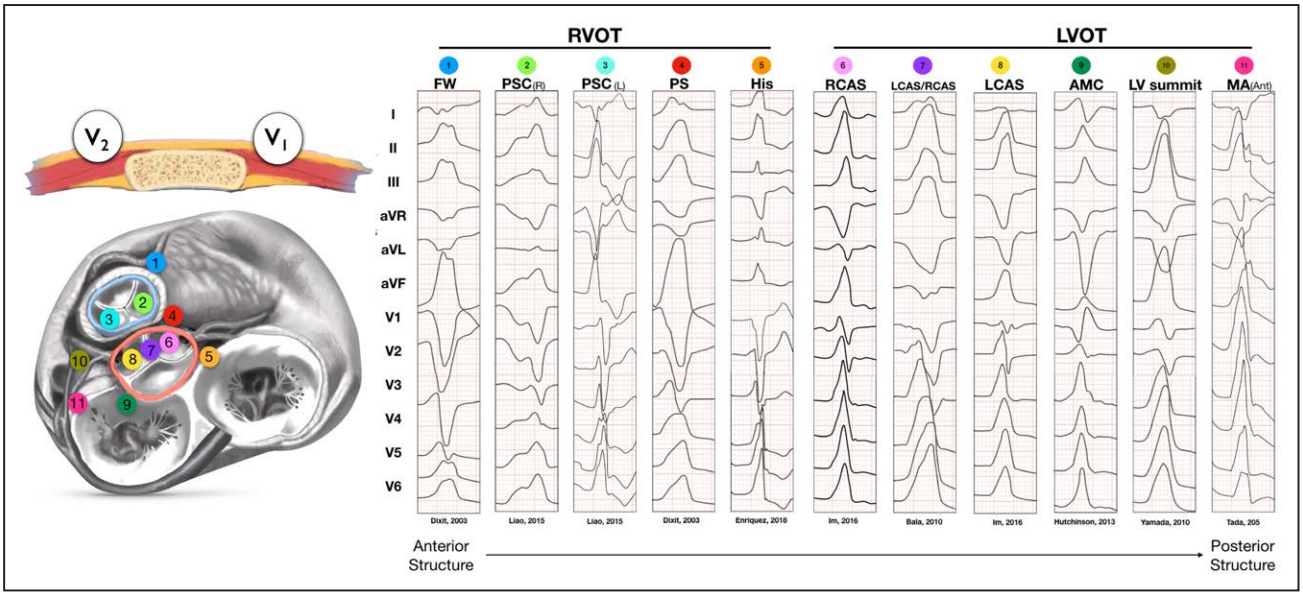

Figure 2. Typical premature ventricular complex (PVC) 12-lead ECG morphologies from common outflow tract sites.
Sagittal image of typical outflow tract sites (**left**, labeled 1–11) with the characteristic 12-lead morphologies for each of the outflow tract PVCs (**right**) as described from seminal studies. AMC indicates aortomitral continuity; FW, free wall; LCAS, left coronary aortic sinus; LV, left ventricular; LVOT, left ventricular outflow tract; MA_{Ant}, anterolateral mitral annulus; MV, mitral valve; PS, posteroseptal; PSC_L, left pulmonary sinus cusp; PSC_R, right pulmonary sinus cusp; RCAS, right coronary aortic sinus; RVOT, right ventricular outflow tract; and TV, tricuspid valve.

presence of Purkinje-like conduction tissue.[34] Arrhythmogenic foci originating below the aortic valvular sinuses are anterosuperior and more leftward, creating deep S waves in lead I and aVL and taller R-wave amplitude in V_1.[21]

The absence of a S wave in V_6 can be used to help distinguish between AMC and anterior mitral annular sites. In a series of 45 patients with LVOT VT, all AMC sites had monophasic R waves in the precordial leads compared to those with anterior mitral annular foci who exhibited an Rs pattern in the precordial leads (with longer intrinsicoid deflection times),[20] suggesting ventricular activation from the AMC is directed anteriorly only due to its position between the left and right fibrous trigone.[22] Furthermore, pacing from the AMC produced a qR pattern that was not seen in any other LVOT site. This unique morphology is due to the initial leftward electrical activation from the left fibrous trigone.[17]

The posterior positioned anterolateral mitral annulus is distant from the precordial leads explaining the typical right bundle branch block (RBBB) pattern in V_1 and positive precordial concordance. Compared to septal sites, pacing from this site produces late notching in the inferior leads and a long QRS duration and negative vector in lead I.[23]

LV Summit VT

The LV summit is the most superior portion of the epicardial LV (as shown in Figure 4B, star) and accounts for ≈12% of OTVAs.[35] It is bounded by the triangle of Brocq and Mouchet: left anterior descending artery, left circumflex artery, and an arc from the left anterior descending superior to the first septal perforating branch anterior to the left circumflex artery laterally (Figure 4A).[36,37] The base of the summit is intersected by the great cardiac vein into a lateral accessible zone (dotted yellow line) and a superior inaccessible zone (dotted white line) due to the close proximity to coronary arteries and thick layer of pericardial fat.[32]

ECGs clues to an epicardial origin are the same as those used for epicardial scar-related VT; slurring of the initial QRS pseudo delta wave. Typically, an RBBB morphology, as the great cardiac vein becomes the anterior interventricular vein at the interventricular septum (more anterior), it can become an LBBB (Figure 4A). This location at the interventricular sulcus corresponds to the characteristic V_2 pattern break, where the R wave in V_2 is less positive than V_1 and V_3 (and lacks transition).[24] Nagashima et al[25] have demonstrated that a successful endocardial-approached LV summit ablation can be predicted by an initial R wave in lead I, suggesting closer proximity to the endocardium in this subgroup.

Parahisian VT

Parahisian VAs represent ≈3% of all idiopathic VT. The His bundle penetrates the membranous septum through the fibrous body and below the RCAS and noncoronary aortic sinus on the left side to become the left and right bundle branches. The posterior location of this region produces a distinctive ECG pattern[13,14] with a narrow QRS LBBB (with a higher maximum deflection index suggesting an epicardial origin), inferior axis (R wave in lead II larger than lead III) and early precordial

Downloaded from http://ahajournals.org by on May 28, 2022

Table 1. Common Sites of OTVA Matched to Characteristic ECG Features

Location of Ventricular Tachycardia	BBB	Frontal Axis	Precordial Transition	V_1	V_6	Lead I	Other Features
Right ventricle—RVOT							
1. Free wall (anterior)[6–8]	LBBB	Inferior	$\geq V_3$	rS	R	rS	Late transition, broad, notched inferior leads, and negative lead I
2. PSC (RC)[9–11]	LBBB	Inferior	$\geq V_3$	rS	R	R	Tall R wave in lead I, small q-wave aVL/aVR ratio
3. PSC (LC)[9–11]	LBBB	Inferior	$\geq V_3$	rS	R	S	Negative lead I, tall, larger q-wave aVL/aVR ratio, R-wave amplitude inferiorly
4. Septal (posterior)[12]	LBBB	Inferior	$\leq V_3$	rS	R	R	Earlier transition
5. Parahisian[13,14]	LBBB	Inferior	$>V_3$	QS	R	R	Isoelectric or positive aVL, large R-wave amplitude in I, V_5 and V_6, tall inferior R wave (II>III)
Left ventricle—ASOV							
6. LCAS/RCAS junction[15,16]	LBBB	Inferior	V_3	qrS	R	R/Rsr′	Notched on the downward deflection in V_1
7. LCAS[3,17,18]	LBBB	Inferior	$\leq V_2$	rS, RS	R	rS	Notched M or W in V_1, QS or RS in lead I
8. RCAS[3,19]	LBBB	Inferior	$\leq V_3$	rS, RS	R	R	Early transition, broad R-wave in V_2
Left ventricle—annular							
9. AMC[20–22]	RBBB	Inferior	None	qR	R	R/Rs	Positive precordial concordance and no S wave in V_6
11. Anterolateral MA[23]	RBBB	Right inferior	Early	R	Rs	rS	Late phase notching of the QRS in the inferior leads
Epicardial							
10. AIV/GCV junction[24,25]	LBBB	Inferior	Early	rS/QS	R	rS	Precordial pattern break (abrupt loss of R wave in V_2), slurred intrinsicoid deflection (pseudodelta)
Crux[26,27]	RBBB	Left superior	Early	Variable	R	Rs	Positive concordance V_2 through V_6, slurred intrinsicoid deflection

AIV indicates anterior interventricular vein; AMC, aortomitral continuity; ASOV, aortic sinus of Valsalva; BBB, bundle branch block; GCV, great cardiac vein; LBBB, left BBB; LCAS, left coronary aortic sinus; MA, mitral annulus; OTVA, outflow tract ventricular arrhythmia; PSC (LC), left cusp of the pulmonary sinus cusps; PSC (RC), right cusp of the pulmonary sinus cusps; RBBB, right BBB; RCAS, right coronary aortic sinus; RVOT, right ventricular outflow tract; and VT, ventricular tachycardia.

Downloaded from http://ahajournals.org by on May 28, 2022

transition (V_1 typically has a QS pattern). The low and rightward position produces an R waves in aVL (which can be notched) and lead I.

ECG PREDICTION ALGORITHMS

We identified 18 publications describing specific ECG algorithms to differentiate OTVA sites (Table 3). Fourteen studies developed algorithms using the standard ECG configuration (8 studies developed algorithms to separate RVOT/LVOT sites, 3 to distinguish between RVOT sites, 2 studies to predict LVOT sites, and 1 to differentiate LV summit sites) and 4 studies developed algorithms based on alternative ECG configurations. These include R-wave duration index, R/S-wave amplitude index, transition zone (TZ) index, V_2S/V_3R index, and the V_2 transition ratio. Each of these will be explained in Figure 5.

RVOT Versus LVOT

Earliest Onset or First Peak/Nadir in V_2

If V_2 has the earliest QRS onset or peak/nadir in the PVC, it predicts an RVOT focus, whereas a later onset in V_2 or later initial peak/nadir in the inferior leads predicts an aortic valvular sinus origin.

Yang et al[38] studied 45 patients with OTVA (LBBB and inferior axis VT), where the earliest onset in any of the 12 leads and the initial peak or nadir of the QRS complex in each lead was measured. V_2 showed the earliest QRS onset in the RVOT compared to aortic sinus group and was strongly predictive of an RVOT focus with a sensitivity of 92% and specificity of 88%. It is hypothesized that the closer anatomic location of the RVOT makes the onset and initial vector earlier than the aortic sinuses.[38]

R-Wave Duration Index and R/S-Wave Amplitude

Using V_1 and V_2, if the R-wave duration index (dividing R-wave/QRS duration of the PVC) is <0.5 and R/S-wave amplitude index (calculated as the greater value of the R/S-wave amplitude ratio in V_1 or V_2) is <0.3, the OTVA is an RVOT origin (Figure 5A and 5B). This was tested in 88 patients with a sensitivity of 88% and specificity of 95%[40] and 15 patients where it was found to predict an RVOT origin.[3]

V_3 R-Wave Deflection Interval and V_1 R-Wave Amplitude

In clinical practice, it is often difficult to predict the site when the precordial transition is at V_3 (Figure 5C).[49] Cheng et al[39] demonstrated that V_3 transition was com-

Table 2. Key Morphological Features Corresponding to Each Anatomic Outflow Tract Site

Site	Key Morphological ECG Feature(s)
RVOT	
Free wall	Late transition, inferior notching
PSC (RC)	Taller R wave in lead I, smaller aVL/aVR ratio
PSC (LC)	Negative lead I, taller R-wave amplitude inferiorly
Posteroseptal	Positive lead I, aVR more negative than aVL
Parahisian	Narrow LBBB, QS in V_1, voltage lead II>III
LVOT	
RCAS	Early transition and rS in V_1
LCAS/RCAS	QS notch in V_1 and V_3 transition
LCAS	Multiphasic M or W in V_1
Aortomitral continuity	qR in V_1 with positive precordial concordance
LV summit	V_2 pattern break, negative lead I, more negative aVL>aVR
LV septal	Narrow LBBB, QS ratio lead II and III >1
Anterolateral MA	Late phase notching in the inferior leads

LBBB indicates left bundle branch block; LCAS, left coronary aortic sinus; LV, left ventricle; LVOT, left ventricular outflow tract; MA, mitral annulus; PSC (LC), left cusp of the pulmonary sinus cusps; PSC (RC), right cusp of the pulmonary sinus cusps; RCAS, right coronary aortic sinus; and RVOT, right ventricular outflow tract.

mon and present in 38% of patients. They developed an algorithm using V_3 R-wave deflection interval >80 ms and V_1 R-wave amplitude >0.3 to predict LVOT VT and if these were not fulfilled it predicted RVOT VT. In 12 patients with V_3 transition, the sensitivity was 100% and specificity of 83% in predicting an RVOT origin. The more posterior positioned LCAS resulted in later precordial transition (>V_3) in 30% of patients with origins from this site. In comparison, the more anteriorly positioned RCAS transitioned <V_3.

V_2 Transition Ratio

Betensky et al[41] developed the V_2 transition ratio in sinus rhythm and the PVC (calculated as R-wave/QRS amplitude in the PVC divided by R-wave/QRS amplitude in sinus rhythm), where a ratio ≥0.6 predicted LVOT origin with a sensitivity of 95% and specificity of 100% and accuracy in 21 prospective cases of 91% (Figure 4E). A greater V_2 transition ratio has also been shown to predict unsuccessful RVOT ablation.[50]

To simplify the algorithm, a more practical approach was formulated: if the PVC transition was later than SR transition, it predicted an RVOT site with 100% specificity and corrected for cardiac rotation.

TZ Index

The TZ is defined as the precordial lead, where the ratio of the R/S-wave amplitude during SR or PVC is between 0.9 and 1.1. A TZ score is calculated based on the precordial lead, where R/S transition occurs in SR and PVC (eg, if in TZ in SR of V_2, 2 points assigned; if the TZ occurred between 2 precordial leads 0.5 was deducted from the latter lead—eg, between V_2 and V_3, 2.5 points assigned).

The TZ index is calculated as the TZ score (PVC) minus TZ score (SR) with an index <0 predicting an LVOT site (regardless of cardiac rotation). This was applied to 112 patients and found it was significantly more accurate than R-wave duration and R/S-wave amplitude index to distinguish RVOT from aortic valve VT (Figure 4G).[42]

V_2S/V_3R Index

This is defined as the PVC S-wave amplitude in lead V_2 divided by R-wave amplitude in V_3 (Figure 4D). The longer duration R wave and higher R/S ratio from OTVA originating from the more posterior aortic valvular sinus location, results in a smaller ratio compared to the RVOT.

In 207 patients, a cutoff V_2S/V_3R ≤1.5 predicted an LVOT origin with a sensitivity of 89% and specificity of 94%.[43] A major advantage of this algorithm is its superiority to differentiate the site in patients with a V_3 transition. In a subgroup of 77 patients, the V_2S/V_3R index ≤1.5 had a sensitivity of 94% and specificity of 78%. The previously mentioned and highly accurate V_3 R-wave deflection interval and V_1 R-wave amplitude were not directly compared in this subanalysis of V_3 transition only.

Combined TZ and V_2S/V_3R Index

Recently, the diagnostic accuracy of all of the previously discussed ECG algorithms were prospectively assessed in 207 patients using a standardized mapping and ablation technique (Figure 4F).[44] The most accurate algorithm was the V_2S/V_3R index, followed by the TZ index. Based on a logistic regression analysis, a mathematical formula was created: $Y=-1.15\times(TZ)-0.494\times(V_2S/V_3R)$ which combined both TZ and V_2S/V_3R indexes. If Y≥−0.76 is predicted an LVOT origin. The combined index had the highest Youden index of 0.77 corresponding to a high sensitivity of 90% and specificity of 87% at predicting an LVOT origin. The accuracy of the combined TZ index was superior when compared to 6 previously validated ECG algorithms and also in a subgroup analysis of V_3 transition. In particular, the other indices assessing cardiac rotation (TZ index and V_2 transition ratio) had much lower sensitivities.

S-R Amplitude Difference (d) in V_1 Through V_2 (V_1–V_2 S-Rd)

Kaypakli et al[45] developed an algorithm to differentiate LVOT and RVOT OTVA sites. Their formula was calculated as follows: (V_1S amplitude+V_2S amplitude)–(V_1R amplitude+V_2R amplitude). One hundred twenty-three patients with OTVA were retrospectively analyzed, where a V_1–V_2 S-Rd>1.625 predicted an RVOT site with a sensitivity of 95% and specificity of 85%. The closer anatomic position of the RVOT (compared to the LVOT)

Downloaded from http://ahajournals.org by on May 28, 2022

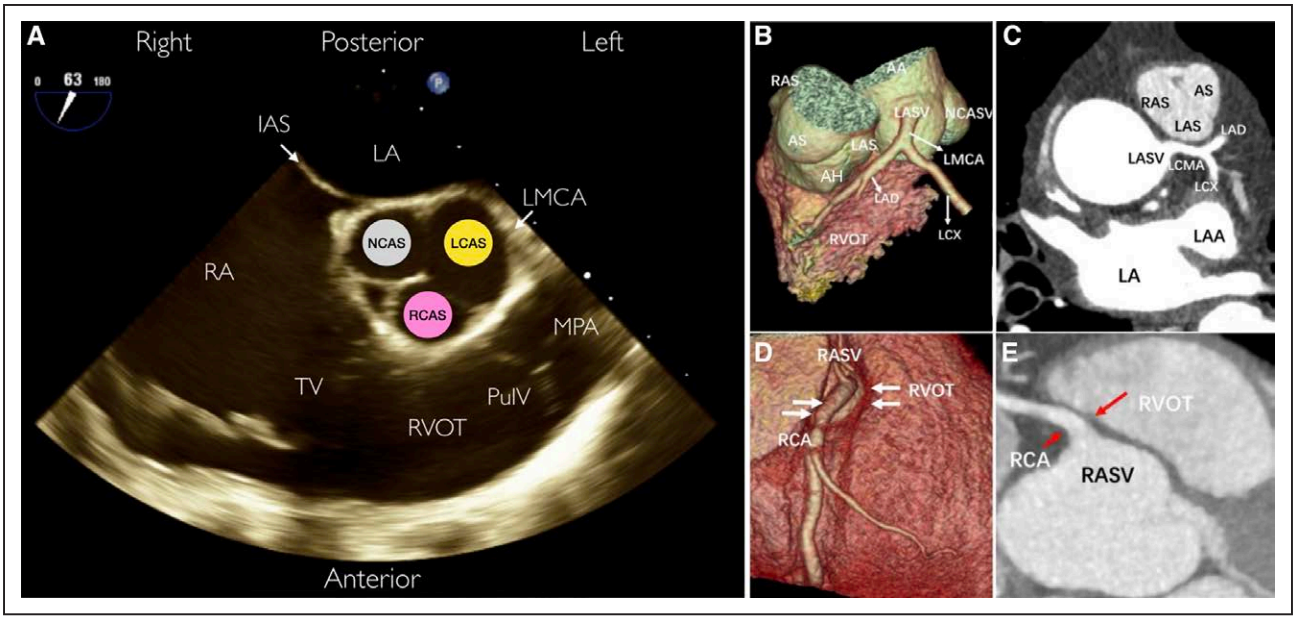

Figure 3. Anatomic relationship of the right- and left-sided outflow tracts.
A, Mid-transesophageal short-axis view demonstrating anatomic position of right ventricular outflow tract (RVOT)/pulmonary valve (PV) with the aortic valvular sinuses. The right coronary aortic sinus (RCAS) and left coronary aortic sinus (LCAS) are positioned closer to the RVOT and PV compared to the noncoronary aortic sinus (NCAS) which is positioned posterior and in close proximity to the intraatrial septum (IAS). **B** and **C**, Left anterior view and axial computed tomographic (CT) image demonstrating relationship between aortic and PVs and the left coronary system. The different craniocaudal levels of the pulmonary valvular sinuses are seen: left cusp (LC) most inferior and anterior cusp (AC)/right cusp (RC) more superiorly. The left main coronary artery (LMCA) exits ≈20 mm above the left aortic sinus of Valsalva (ASOV) between the main pulmonary artery and left auricle before entering the coronary sulcus and bifurcating into the left anterior descending (LAD) and left circumflex artery (LCx) arteries. The LAD continues around the left side of the pulmonary artery then descends obliquely towards the apex via the anterior interventricular sulcus. **D** and **E**, Right lateral view and axial CT image demonstrating relationship of the RC of the RVOT and right coronary artery (RCA). The RC has also been shown to be <5 mm of the RCA (most commonly proximal) in 82% of patients.[30] AH indicates anterior horn (of RV); AS, anterior sinus; LA, left atrium; LAS, left adjacent sinus; LASV, left aortic sinus of Valsalva; MPA, main pulmonary artery; NCASV, noncoronary aortic sinus of Valsalva; RA, right atrium; RAS, right adjacent sinus; RASV, right aortic sinus of Valsalva; and TV, tricuspid valve. **B**–**E**, Adapted from Dong et al[30] with permission. Copyright © 2018, John Wiley and Sons.

to V_1 and V_2, result in a larger amplitude in the S wave in those leads from this site. The more posterior LVOT will generate a larger amplitude in the R wave at these sites. Hence, the V_1–V_2 S-Rd is a measure of the proximity of the impulse foci from V_1 and V_2.

Septal Versus Free Wall RVOT

PVC-QRS Duration/QRS Duration of the Preceding Sinus Beat

Further delineation with the RVOT location was developed in an algorithm.[46] If transition was greater than V_4 or the R-wave duration index or R/S amplitude index pointed towards the RVOT a further step was introduced to distinguish between septal and free-wall sites. If the QRS duration of the PVC divided by the QRS of the sinus beat ≥1.9, this suggests a free-wall site.

Anterolateral Mitral Annulus

Inferior R-Wave Polarity and Notching

Kumagai et al[48] devised an algorithm to localize mitral annular idiopathic VT in 35 patients. Those with early precordial transition (V_1 or V_2), S wave in V_6, inferior axis (positive inferior leads) and an R wave in avF ≥1.6 mV predicted an anterolateral site.

LV Summit

Accessible Versus Inaccessible LV Summit Sites

ECG algorithms have also been developed to assist in distinguishing LV summit site that are outside the ablation inaccessible zone and within the more lateral accessible zone (Figure 5). An RBBB, TZ <V_1, aVL/aVR ratio >1.1 and S wave in V_5 or V_6 predicted whether an LV summit OTVA could be ablated in the accessible area.[35]

ECG ALGORITHMS USING ALTERNATIVE ECG CONFIGURATIONS

We identified 4 studies that have used alternative ECG positions to improve the diagnostic accuracy of predicting OTVA origin.

VIRTUAL RIGHT-SIDED LEADS

The use of right-sided precordial leads has been recently described by Nakano et al.[51] Virtual synthesized right-sided leads/waveforms (Syn-V_3R, Syn-V_4R, Syn-V_5R) were generated. In their study, 63 patients who had undergone successful OTVA ablation were studied.[51] In

Downloaded from http://ahajournals.org by on May 28, 2022

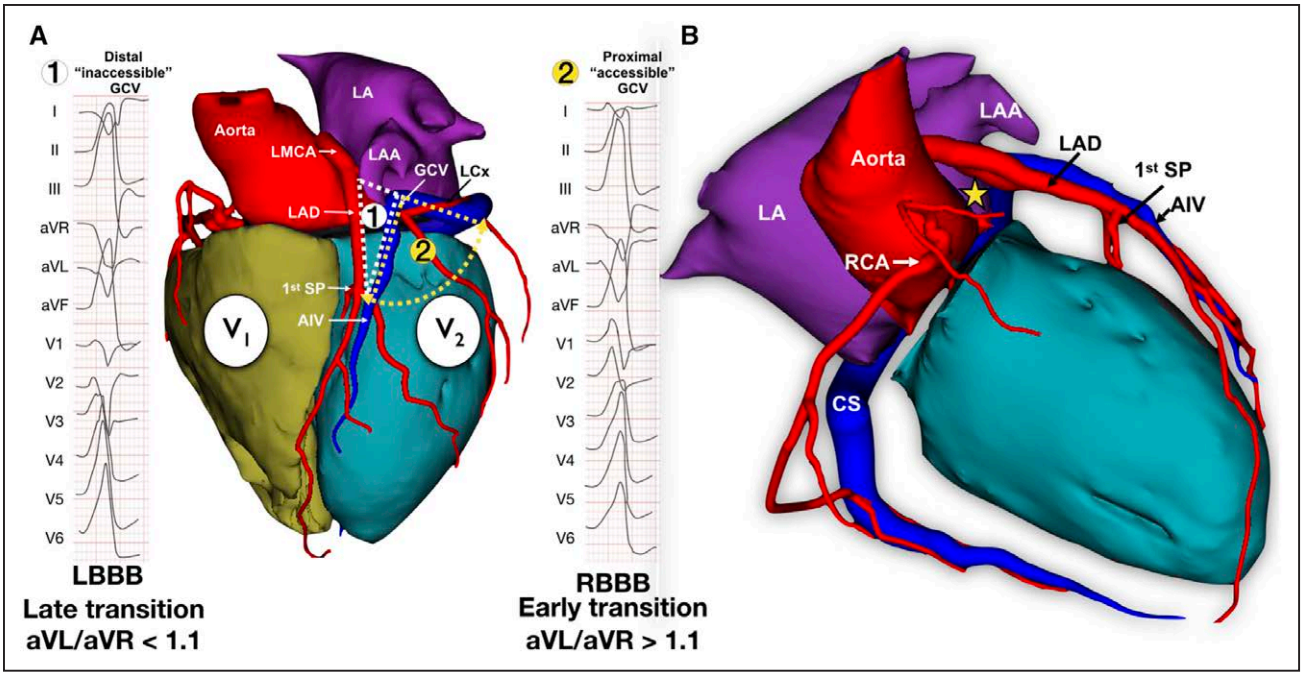

Figure 4. Left ventricular (LV) summit: boundaries, anatomic landmarks, and typical ECG morphologies.
The LV summit is the most superior portion of the LV (star, **B**) and an important anatomic landmark as it is the region on the epicardial surface, where the left main coronary artery (LMCA) bifurcates and is recognized as the commonest source of idiopathic epicardial ventricular arrhythmias (VAs).[35] Anatomic landmarks defining the LV summit are divided into an accessible zone at the proximal great cardiac vein (GCV; dotted yellow line) and inaccessible zone at the distal GCV (dotted white line; **A**). The inaccessible zone is less likely to be a successful site of ablation due to overlaying perivascular fat and additional risk of left coronary injury. Characteristic ECG morphologies for these sites as described by[37] demonstrate the typical right bundle branch block (RBBB) in the proximal accessible zone with reversal of R-wave transition in V_1 (left bundle branch block [LBBB]) at a more distal GCV site in the inaccessible zone. AIV indicates anterior interventricular vein; CS, coronary sinus; LA, left atrium; LAA, left atrial appendage; LAD, left anterior descending; LCx, left circumflex artery; LMCA, left main coronary artery; RCA, right coronary artery; and SP, septal perforator. Adapted from Baman et al[37] with permission. Copyright © 2010, American Heart Association, Inc.

Downloaded from http://ahajournals.org by on May 28, 2022

all of the RVOT free wall VTs, there was no R/S transition (sensitivity of 100% and specificity of 85%), whereas in all of the LVOT VT there was R>S concordance (sensitivity and specificity of 100%). In the remaining septal RVOT cases, a R/S transition was seen in the majority of cases. R>S in all synthesized right-sided leads could be used to distinguish LVOT from RVOT sites. An additional pacemapping study also using synthesized right-sided leads found V_5R morphology pattern was able to predict OTVA. Specifically, a Rs or rS pattern in this lead predicted RVOT origin with 87% sensitivity and 91% specificity.[52]

HIGH PRECORDIAL V_1 THROUGH V_2 LEAD POSITIONS

Mimicking the superiority of the improvised lead positioning in the diagnosis of Brugada syndrome,[53] altering the vertical position of V_1 and V_2 has also been studied in OTVA localization.[54] In a group of 34 patients, moving from the fourth to the third (superiorly) or the fifth (inferiorly) intercostal space altered the R/S ratio of OTVA significantly. Superior displacement reduced the R-wave amplitude, resulting in a decrease in R/S ratio. Conversely, inferior displacement increased R-wave amplitude, increasing the R/S ratio. The change in precordial transition lead to errors in site prediction as the increased ratio (inferior position) suggested LVOT origin in patients with RVOT foci and those with a decreased ratio (superior position) pointed to an RVOT site when the arrhythmia was originating from the LVOT.

V_4/V_8 INDEX

Recently, an algorithm modifying the precordial V_5 to a posterior position (V_8), just left of the spine at the same level has been created.[55] Using the V_4/V_8 index (dividing V_4/V_8 ratio of the PVC by the V_4/V_8 ratio in sinus rhythm), this allowed the anteroposterior ratio to be calculated and was able to differentiate left- and right-sided OTVA with high predictive accuracy in a prospective cohort (n=40 patients) with a specificity of 96% and positive predictive value of 89%.[55] Right-sided PVCs had significantly lower V_4/V_8 ratios compared to left-sided foci (2.3±2.4 versus 11.7±10.6, $P<0.001$, respectively). Using a cutoff of >2.28, the V_4/V_8 index had a sensitivity of 67%, specificity of 98%, and positive predictive value of 89% to predict left-sided OTVA. The V_4/V_8 index was more accurate when compared to the V_2 transition ratio, V_2S/V_3R and a selective group that transitioned at V_3.

Table 3. Summary of the Published Algorithms and the Predictive Valve Used to Differentiate RVOT and LVOT OTVA

	Site	Patients	Study Type	Algorithm Used	Predictive Value
Yang et al[38]	RVOT/LVOT	45	Retrospective and multicenter	Earliest onset of QRS and peak/nadir in V_2 predicting RVOT origin	Sensitivity 92%; specificity 88%
			Males: 16 (35)		
			Mean age: 41±14		
			EAM: 31 (68)		
Cheng et al[39]	RVOT/LVOT	42	Retrospective (n=31), prospective (n=11), and single-center	V_3 transition: R-wave deflection interval in V_3 (>80 ms) and R-wave amplitude index in V_1 (>0.3) predicting LVOT origin	Sensitivity 100%; specificity 83%
			Males: 11 (35)		
			Mean age: 45±18		
			EAM: NR		
Ito et al[40]	RVOT/LVOT	168	Retrospective (n=80), prospective (n=88), and single-center	S-wave amplitude V_6 and transition zone in V_4 or S wave in lead I; following this, R/S amplitude index and R-duration index in lead I	RVOT septum 68%; RVOT free wall 81%; RVOT His 73%
			Males: 79 (47)		
			Mean age: 53±15		
			EAM: NR		
Betensky et al[41]	RVOT/LVOT	61	Retrospective (n=40), prospective (n=21), and single-center	V_2 transition ratio ≥0.6 predicting LVOT origin	Sensitivity 95%; specificity 100%
			Males: 19 (48)		
			Mean age: 44±14		
			EAM: 61 (100)		
Yoshida et al[42]	RVOT/LVOT	112	Retrospective and single-center	Transition zone index <0 predicting LVOT origin	Sensitivity 88%; specificity 82%
			Males: 56 (50)		
			Mean age: 48±17		
			EAM: 25 (22)		
Yoshida et al[43]	RVOT/LVOT	207	Retrospective and multicenter	V_2S/V_3R index ≤1.5 predicting LVOT origin	Sensitivity 89%; specificity 94%
			Males: 83 (40)		
			Mean age: 48±16		
			EAM: 207 (100)		
He et al[44]	RVOT/LVOT	695	Retrospective (n=488), prospective (n=207), and single-center	Combined TZ index and V_2S/V_3R, $Y=-1.15\times(TZ)-0.494\times(V_2S/V_3R)$. If ≥−0.76 predicts LVOT origin	Sensitivity 90%; specificity 87%
			Males: 158 (32)		
			Mean age: 41±13		
			EAM: NR		
Kaypakli et al[45]	RVOT/LVOT	123	Retrospective and single-center	V_1–V_2 S-R difference=$(V_1S+V_2S)-(V_1R+V_2R)$. If >1.625 predicted RVOT origin	Sensitivity 95%; specificity 85%
			Males: 70 (57)		
			Mean age: 46±13		
			EAM: 22 (18)		
Joshi et al[8]	RVOT (septal vs free wall)	46	Prospective and single-center	QRS duration ≥140 ms and R wave, notching in inferior leads and V_3 R/S ratio ≤1 predicting free-wall origin; following this, lead I (to determine anterior or posterior) and aVL (to determine caudal or cranial)	Sensitivity 74%; specificity 93%
			Males: NR		
			Mean age: NR		
			EAM: 46 (100)		
Dixit et al[12]	RVOT (septal vs His vs free wall)	14	Prospective and single-center	Notching in the R waves in the inferior leads and R≥S in V_4 predicting free-wall origin	RVOT septum 41%; RVOT free wall 72%; RVOT His 53%
			Males: 8 (57)		
			Mean age: 44±13		
			EAM: 14 (100)		

(*Continued*)

Downloaded from http://ahajournals.org by on May 28, 2022

Table 3. Summary of the Published Algorithms and the Predictive Valve Used to Differentiate RVOT and LVOT OTVA

	Site	Patients	Study Type	Algorithm Used	Predictive Value
Zhang et al[46]	RVOT (septal vs free wall)	65	Retrospective (n=52), prospective (n=13), and multicenter Males: 21 (40) Mean age: 42±14 EAM: 65 (100)	LBBB/inferior axis→transition zone ≥V_4→absence of an RR′ or RSR′ in aVL→PVC duration/sinus beat duration ≥1.9 predicting free-wall origin	RVOT septum 79%; RVOT free wall 92%; RVOT His 88%
Yamada et al[35]	LV (summit)	27	Retrospective and multicenter Males 13 (48) Mean age: 46±11 EAM: NR	Accessible site prediction (cured by ablation in the GCV, AIV region): RBBB pattern (transition zone earlier than V_1), aVL/aVR amplitude ratio >1.1, and S wave in V_5 or V_6	Sensitivity 87%; specificity 100%
Ouyang et al[3]	LVOT (aortic valvular sinus)	15	Retrospective and single-center Males: 8 (53) Mean age: 36±20 EAM: NR	R/S amplitude index (>0.5) and R-duration index (>0.3) predicting LVOT	Statistically significant compared with RVOT origin
Li et al[26]	LVOT (ISP)	7	Retrospective and multicenter Males: 5 (71) Mean age: 60±14 EAM: 7 (100)	ISP site prediction: RBBB, transition in V_2, left superior axis, and small S wave in V_6	Not assessed
Tada et al[47]	Anterolateral MA	19	Prospective and single-center Males: 10 (52) Mean age: 61±12	Anterolateral MA prediction: precordial transition <V_2 and R or Rs in V_2 through V_5, positive QRS vector inferiorly and notching of the R wave in the inferior leads	Sensitivity 60%; specificity 99.7%
Kumagai et al[48]	Anterolateral MA	35	Prospective and single-center Males: 24 (69) Mean age: 53±14	Anterolateral MA prediction: precordial transition V_1 or V_2, S wave in V_6, positive R-wave inferiorly, and R wave ≥1.6 mV aVF	85% accuracy

AIV indicates anterior interventricular vein; GCV, great cardiac vein; EAM, electroanatomical mapping; ISP, inferoseptal process; LBBB, left bundle branch block; LVOT, left ventricular outflow tract; MA, mitral annulus; NR, not recorded; OTVA, outflow tract ventricular arrhythmia; PVC, premature ventricular complex; RBBB, right bundle branch block; RVOT, right ventricular outflow tract; and TZ, transition zone.

Downloaded from http://ahajournals.org by on May 28, 2022

V_3R/V_7 INDEX

Modifying the standard precordial leads to create a right-sided (V_3R) lead and posterior lead (V_7) has been recently shown to successfully differentiate RVOT from LVOT sites with high accuracy. Cheng et al[56] demonstrated a V_3R/V_7 index ≥0.85 (n=97 patients) predicted an LVOT origin with 87% sensitivity and 96% specificity and prospectively validated their index in a further 94 patients with a 98.6% accuracy. The area under the curve was highest for the V_3R/V_7 index (0.95) compared to V_2S/V_3R (0.89), V_2 transition ratio (0.79) and lowest for the TZ index (0.66). It was also shown to have the highest accuracy in subanalyses in those with cardiac rotation or transition at V_3.

An algorithm guiding clinicians to the SOO of OTVA incorporating ECG prediction algorithms (standard or alternative ECG configurations) with typical ECG signatures is shown in Figure 6.

ANATOMIC CONSIDERATIONS AND PITFALLS OF CLASSICAL ECG SIGNATURES

The OT is a complex and anatomically condensed region with overlaying critical structures in close proximity. The use of typical ECG rules to identify the SOO may erroneously point to an alternative site, distinct from the arrhythmogenic foci. SOO prediction is important before catheter mapping and ablation potentially being able to hone in on the region of interest, limiting unnecessary mapping and ablation. It also has implications for disclosing additional risks to patients preprocedurally, procedural factors, and anticipated procedural success. Furthermore, non-RVOT sites are more likely to develop PVC-induced cardiomyopathy[57] and are at higher risk of cardiac events due to greater variations in coupling interval.[58]

ECG signatures are typically based on classical morphological characteristics using the bundle branch pattern in V_1 and precordial transition. Activation from anterior structures such as the free wall of the RVOT will have LBBB morphology due to the net electrical forces propagating away from this site. Conversely, activation from posteriorly located structures such as the mitral annulus will have RBBB pattern morphology as the net activation forces are toward V_1. In general, there is a gradual progression in V_1 morphology from a complete LBBB to an RBBB as the SOO shifts from anterior to posteriorly directed structures (ie, anterior RVOT to

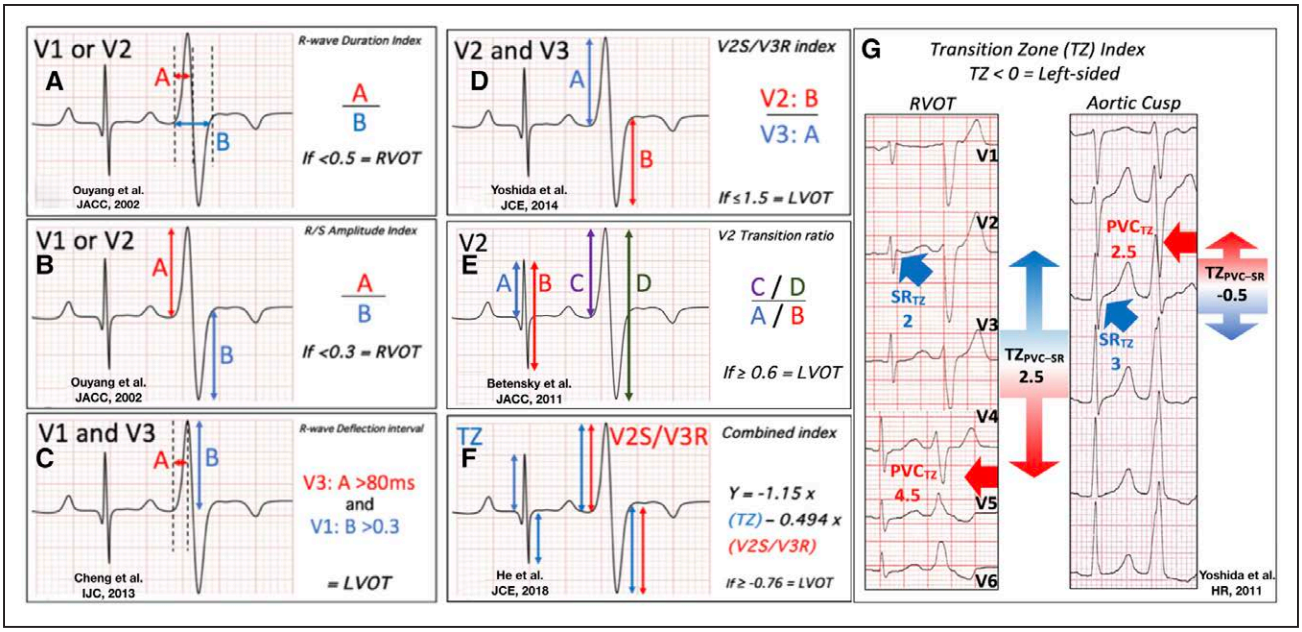

Figure 5. ECG prediction algorithms used to differentiate right and left-sided outflow tract ventricular arrhythmia (OTVA) origins.
From **top** to **bottom**, R-wave duration index, V_2S/V_3R index, R/S amplitude index, V_2 transition ratio, R-wave deflection interval, combined index, and transition zone (TZ) index (with an right ventricular outflow tract [RVOT] and aortic valvular sinus example). LVOT indicates left ventricular outflow tract; and PVC, premature ventricular complex.

posterior RVOT, RCAS-LCAS commissure, LCAS, AMC, great cardiac vein/anterior interventricular vein, and LV summit). The only break from this pattern of progression are foci originating from the AMC which have classically have a qR in V_1[17] which may be due to a unique exit from remnant His-Purkinje tissue.[34]

The more anterior RVOT free wall will transition later (V_4 or V_5) than the septal RVOT (V_3 or V_4) which is more

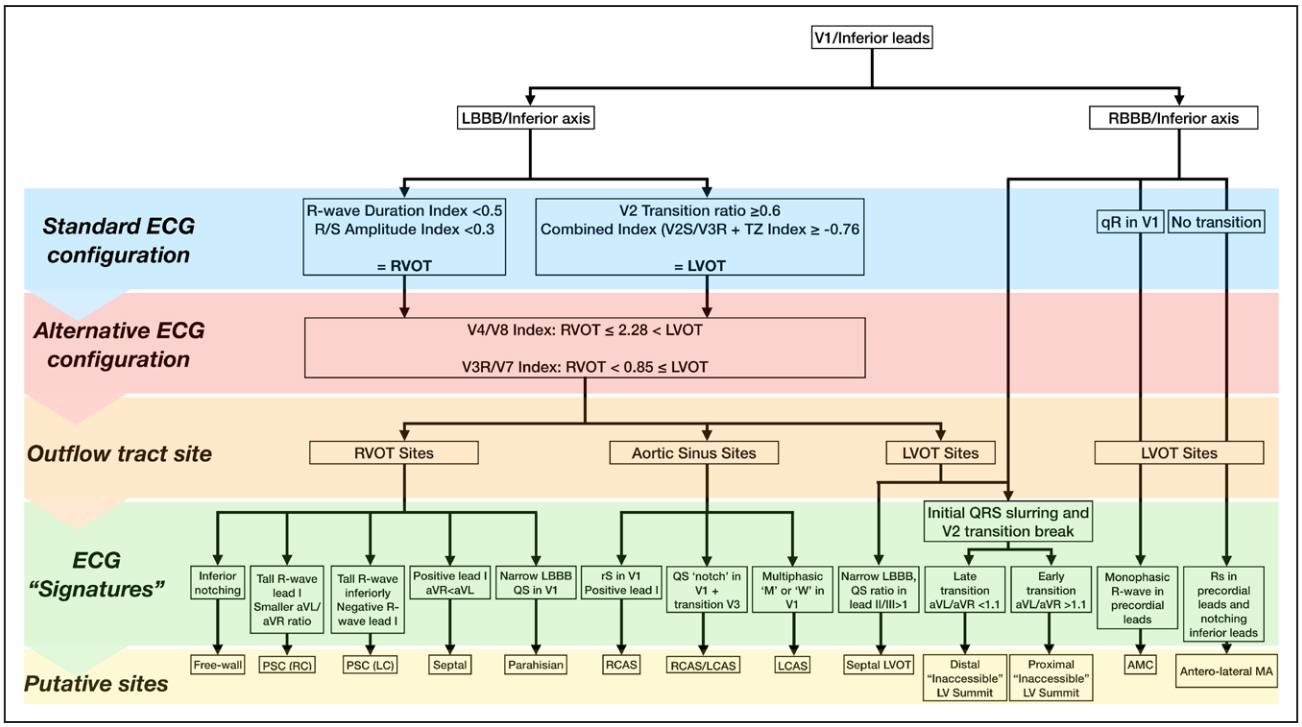

Figure 6. Algorithm guiding localization of outflow tract ventricular arrhythmia (OTVA).
The initial step is to examine V_1 and the inferior leads. If the pattern is a right bundle branch block (RBBB)/inferior axis, this point to a aortomitral continuity (AMC) or anterolateral mitral annulus (MA) site of origin (SOO). A left bundle branch block (LBBB)/inferior axis allows application of ECG prediction algorithms (either standard or alternative ECG configuration can be used) to distinguish between right ventricular outflow tract (RVOT) and left ventricular outflow tract (LVOT) sites. Typical morphological signatures can be applied to position the SOO to a putative site. LCAS indicates left coronary aortic sinus; PSC (LC), left cusp of the pulmonary sinus cusps; PSC (RC), right cusp of the pulmonary sinus cusps; and RCAS, right coronary aortic sinus.

Downloaded from http://ahajournals.org by on May 28, 2022

posterior (Figure 2; Tables 1 and 2). Similarly, the anteriorly positioned RCAS (directly posterior to the septal or posterior RVOT) will transition later (V_2 or V_3) than those arising from the posterior LCAS (R wave typically seen in V_1) with a multiphasic morphological appearance (W or M)[18,32] (Figure 2; Tables 1 and 2). A QS notch in V_1 and transition at V_3 is typically seen with an origin at the RCAS-LCAS junction (Figure 2; Tables 1 and 2).[15] The absence of an intrinsicoid deflection, precordial lead monophasic R wave, and absence of an S wave in V_6 suggests a SOO in the aortic sinuses as opposed to the AMC or anterior mitral annulus.[20]

These ECG signatures are simple to use, however, are inaccurate to locate specific sites within each side of the tracts, particularly if transition occurs at V_3. Furthermore, these studies are based on only limited patient numbers, reducing their generalizability. More detailed analyses have predominantly correlated morphology to pacemapping, however, the major limitation of pace mapping is the risk of remote ventricular pacing (far-field capture). Prior studies mapping idiopathic RVOT VT patients have shown the spatial resolution of pacemapping to be inferior to activation mapping.[59,60]

The deficiencies in accurate morphological assessment of OTVA foci prediction led to the development of a multitude of algorithms. Similar to the morphology studies, a pitfall of algorithm-prediction studies are limited patient numbers. Nonetheless, these algorithms have particularly focused on separating right-sided and left-sided OTVA by utilizing the smaller R-wave amplitude and shorter durations that are seen in RVOT foci. Anatomically, RVOT foci are more anterior (and closer) to V_1 and V_2. This explains why the initial vector moving away from the anterior site will have smaller R-wave duration and amplitude compared to aortic sinus vector which will activate more myocardium (and take a longer time, hence larger R-wave duration index) from the central location to the anterior wall. Interestingly, in the description by Ito et al,[40] there was no overlap in ratios using their cutoffs comparing septal RVOT and RCAS sites, despite their close anatomic proximity. One explanation for this is the fact that the posterior RVOT is not strictly septal but is formed by the ventriculo-infundibular fold with an extracardiac tissue plane that can be seen in Figure 1 (yellow arrows).

DISADVANTAGES OF ECG PREDICTION ALGORITHMS

An issue encountered with published algorithms is the chance of calculation errors which can be perpetuated by the intricate, computational method to derive measurements and multiple steps making it difficult to easily calculate. Indeed, a recent study compared 2 of the more easily applicable algorithms (Dixit et al[12] and Joshi et al[8]) to more complicated algorithms (Zhang et al[46] and Ito et al[40]) in 99 patients with RVOT tachycardias.[61] The latter had a higher predictive accuracy at the detriment of more intricate steps and more difficult to use in routine clinical practice.

A limitation of early developed algorithms was the inability to correct for cardiac rotation which is commonly present even in a cohort of patients with predominantly structurally normal hearts. This has led to the development of the V_2 transition ratio and TZ index which take into account cardiac axis variation, respiratory variation and ECG lead position to normalize precordial transition. This involves not only calculating the absolute transition of the PVC, but correcting it to the sinus rhythm precordial transition. Yoshida et al[42] demonstrated that cardiac malrotation of the electrical axis is common. Thirty-seven percent of their cohort had counter-clockwise rotation (defined as SR TZ $<V_3$) and 13% had clockwise rotation (defined as an SR TZ $>V_4$). Other factors that influence the predictive accuracy of algorithms include lead positions, aorta deformities, chest wall thickness (ie, obesity, chest wall deformity), medications, ventricular hypertrophy, and preferential conduction.[42,62]

Another factor that may reduce the accuracy of ECG predictive algorithms in the OT is the finding that some patients with aortic valvular sinus arrhythmias have preferential conduction to the RVOT with early breakout at this site, possibly due to myocardial fiber orientation or shared muscle. The posterior subpulmonic valve is positioned in close proximity to the anterior subaortic LVOT and distal RCAS; whereas parts of the aortic valvular sinuses (eg, the lateral and distal LCAS) are adjacent to the RVOT.[4] The possibility of shared myocardial connections bridging left and right OTs (with different exits) has clinical implications as it may allow for alternative CA approaches (including from the other OT) to be used in failed or challenging cases. Yamada et al[62] demonstrated that ≈25% of patients with OTVA originating from the aortic sinuses (as determined by earliest activation site) had better pacemap match in RVOT breakout sites compared to aortic sinus sites. Furthermore, a significantly longer stimulation-QRS interval was present when pacing the RVOT compared to the aortic sinuses suggestive of fiber extensions connecting the aortic sinus to the RVOT or LV septum exist in some patients. When mapping the posterior RVOT, the presence of early but far-field signals may be the result of preferential conduction through bridging fibers from a deeper LVOT focus. Ablation at the early RVOT site may fail to eliminate the focus despite the presence of an excellent pacemap. Mapping the adjacent LVOT may result in equally early but near-field signals which result in successful ablation. Conversely, a poor pacemap match may be encountered at the site of earliest activation due to preferential conduction of the paced

Downloaded from http://ahajournals.org by on May 28, 2022

beat away from the putative focus to a remote exit site. In this situation, careful interrogation looking for the earliest near-field signal in the region of interest may be more useful than pacemapping.[4] It has also recently been shown that 4% of patients with OTVA have a change in preferential exit following initial RF delivery associated with alteration of the original ECG morphology to an adjacent site.[63] Ablation at the new earliest site eliminated ectopy in 88%, possibly suggestive of an intramural VA origin with a shift in the surface breakout due to ablation at the first preferential exit.

Finally, alternative ECG configurations can be used to maximize the largest deviations in vector ratios and may improve the prediction accuracy beyond what can be achieved using conventional configurations. Relatively small lead displacements in the anterior precordium have been to significantly alter the transition vector ratio.[54] Furthermore, V_4 through V_6 are distinctly distant from these sites (lateral and lower) and are of limited value in differentiating OTVA subtypes as precordial transition is most discriminatory between V_1 and V_3. The synthesized right-sided leads are useful as they offer binary differentiation between RVOT and LVOT foci. Future expansion of this study to include all subtypes of LVOT foci is desired. Other novel configurations such as the V_4/V_8 index and V_3R/V_7 indices are highly specific and particularly strengthened by a large validation cohorts, corrected to cardiac rotation, and accurately differentiate those with a V_3 transition.

CONCLUSIONS

Ablation outcomes can be improved if the OTVA origin can be predetermined before CA. Differentiating left-sided and right-sided OTVA can be predicted with a variable accuracy using the ECG algorithms before CA. A combined model using the TZ index and V_2S/V_3R is the most accurate, but its clinical utility may be limited. Promising novel techniques altering the ECG configuration have been developed and can also be used to predict OTVA with high accuracy.

ARTICLE INFORMATION

Correspondence

Geoffrey Lee, MBChB, PhD, Department of Cardiology, Royal Melbourne Hospital, 300 Grattan St, Parkville, VIC 3050, Australia. Email geoff.lee@mh.org.au

Affiliations

Department of Cardiology, Royal Melbourne Hospital, Faculty of Medicine, Dentistry, and Health Science, University of Melbourne, VIC, Australia (R.D.A., R.P., G.W., A.V., H.S., T.W., P.B.S., J.B.M., A.M., P.M.K., J.K., G.L.). Department of Cardiology, Westmead Hospital, NSW, Australia (S.K.). Westmead Applied Research Centre, University of Sydney, NSW, Australia (S.K.). Department of Cardiology, Alfred Hospital, VIC, Australia (A.V., H.S., A.M., P.M.K.). Baker IDI Heart & Diabetes Institute, Melbourne, VIC, Australia (A.V., H.S., A.M., P.M.K.).

Disclosures

None.

REFERENCES

1. Sirichand S, Killu AM, Padmanabhan D, Hodge DO, Chamberlain AM, Brady PA, Kapa S, Noseworthy PA, Packer DL, Munger TM, Gersh BJ, McLeod CJ, Shen WK, Cha YM, Asirvatham SJ, Friedman PA, Mulpuru SK. Incidence of idiopathic ventricular arrhythmias: a population-based study. *Circ Arrhythm Electrophysiol*. 2017;10:e004662. doi: 10.1161/CIRCEP.116.004662
2. Srivathsan K, Lester SJ, Appleton CP, Scott LR, Munger TM. Ventricular tachycardia in the absence of structural heart disease. *Indian Pacing Electrophysiol J*. 2005;5:106–121.
3. Ouyang F, Fotuhi P, Ho SY, Hebe J, Volkmer M, Goya M, Burns M, Antz M, Ernst S, Cappato R, Kuck KH. Repetitive monomorphic ventricular tachycardia originating from the aortic sinus cusp: electrocardiographic characterization for guiding catheter ablation. *J Am Coll Cardiol*. 2002;39:500–508.
4. Asirvatham SJ. Correlative anatomy for the invasive electrophysiologist: outflow tract and supravalvar arrhythmia. *J Cardiovasc Electrophysiol*. 2009;20:955–968. doi: 10.1111/j.1540-8167.2009.01472.x
5. Saremi F, Ho SY, Cabrera JA, Sánchez-Quintana D. Right ventricular outflow tract imaging with CT and MRI: part 2, function. *AJR Am J Roentgenol*. 2013;200:W51–W61. doi: 10.2214/AJR.12.9334
6. Jadonath RL, Schwartzman DS, Preminger MW, Gottlieb CD, Marchlinski FE. Utility of the 12-lead electrocardiogram in localizing the origin of right ventricular outflow tract tachycardia. *Am Heart J*. 1995;130:1107–1113.
7. Josephson ME, Horowitz LN, Waxman HL, Cain ME, Spielman SR, Greenspan AM, Marchlinski FE, Ezri MD. Sustained ventricular tachycardia: role of the 12-lead electrocardiogram in localizing site of origin. *Circulation*. 1981;64:257–272.
8. Joshi S, Wilber DJ. Ablation of idiopathic right ventricular outflow tract tachycardia: current perspectives. *J Cardiovasc Electrophysiol*. 2005;16(suppl 1):S52–S58. doi: 10.1111/j.1540-8167.2005.50163.x
9. Timmermans C, Rodriguez LM, Medeiros A, Crijns HJ, Wellens HJ. Radiofrequency catheter ablation of idiopathic ventricular tachycardia originating in the main stem of the pulmonary artery. *J Cardiovasc Electrophysiol*. 2002;13:281–284.
10. Tada H, Kurosaki K, Ito S, Naito S, Yamada M, Miyaji K, Hashimoto T, Oshima S, Nogami A, Taniguchi K. Idiopathic premature ventricular contractions arising from the pulmonary artery: importance of mapping in the pulmonary artery in left bundle branch block-shaped ventricular arrhythmias. *Circ J*. 2005;69:865–869.
11. Sekiguchi Y, Aonuma K, Takahashi A, Yamauchi Y, Hachiya H, Yokoyama Y, Iesaka Y, Isobe M. Electrocardiographic and electrophysiologic characteristics of ventricular tachycardia originating within the pulmonary artery. *J Am Coll Cardiol*. 2005;45:887–895. doi: 10.1016/j.jacc.2004.10.071
12. Dixit S, Gerstenfeld EP, Callans DJ, Marchlinski FE. Electrocardiographic patterns of superior right ventricular outflow tract tachycardias: distinguishing septal and free-wall sites of origin. *J Cardiovasc Electrophysiol*. 2003;14:1–7.
13. Yamada T, McElderry HT, Doppalapudi H, Kay GN. Catheter ablation of ventricular arrhythmias originating in the vicinity of the His bundle: significance of mapping the aortic sinus cusp. *Heart Rhythm*. 2008;5:37–42. doi: 10.1016/j.hrthm.2007.08.032
14. Yamauchi Y, Aonuma K, Takahashi A, Sekiguchi Y, Hachiya H, Yokoyama Y, Kumagai K, Nogami A, Iesaka Y, Isobe M. Electrocardiographic characteristics of repetitive monomorphic right ventricular tachycardia originating near the His-bundle. *J Cardiovasc Electrophysiol*. 2005;16:1041–1048. doi: 10.1111/j.1540-8167.2005.40787.x
15. Bala R, Garcia FC, Hutchinson MD, Gerstenfeld EP, Dhruvakumar S, Dixit S, Cooper JM, Lin D, Harding J, Riley MP, Zado E, Callans DJ, Marchlinski FE. Electrocardiographic and electrophysiologic features of ventricular arrhythmias originating from the right/left coronary cusp commissure. *Heart Rhythm*. 2010;7:312–322. doi: 10.1016/j.hrthm.2009.11.017
16. Yamada T, Yoshida N, Murakami Y, Okada T, Muto M, Murohara T, McElderry HT, Kay GN. Electrocardiographic characteristics of ventricular arrhythmias originating from the junction of the left and right coronary sinuses of Valsalva in the aorta: the activation pattern as a rationale for the electrocardiographic characteristics. *Heart Rhythm*. 2008;5:184–192. doi: 10.1016/j.hrthm.2007.09.029
17. Lin D, Ilkhanoff L, Gerstenfeld E, Dixit S, Beldner S, Bala R, Garcia F, Callans D, Marchlinski FE. Twelve-lead electrocardiographic characteris-

Downloaded from http://ahajournals.org by on May 28, 2022

tics of the aortic cusp region guided by intracardiac echocardiography and electroanatomic mapping. *Heart Rhythm*. 2008;5:663–669. doi: 10.1016/j.hrthm.2008.02.009
18. Bala R, Marchlinski FE. Electrocardiographic recognition and ablation of outflow tract ventricular tachycardia. *Heart Rhythm*. 2007;4:366–370. doi: 10.1016/j.hrthm.2006.11.012
19. Im SI, Park KM, Park SJ, Kim JS, On YK. New electrocardiographic criteria for predicting successful ablation of premature ventricular contractions from the right coronary cusp. *Int J Cardiol*. 2016;224:199–205. doi: 10.1016/j.ijcard.2016.09.029
20. Kumagai K, Fukuda K, Wakayama Y, Sugai Y, Hirose M, Yamaguchi N, Takase K, Yamauchi Y, Takahashi A, Aonuma K, Shimokawa H. Electrocardiographic characteristics of the variants of idiopathic left ventricular outflow tract ventricular tachyarrhythmias. *J Cardiovasc Electrophysiol*. 2008;19:495–501. doi: 10.1111/j.1540-8167.2007.01085.x
21. Kamioka M, Mathew S, Lin T, Metzner A, Rillig A, Deiss S, Rausch P, Lemes C, Makimoto H, Hu H, Liang D, Wissner E, Tilz RR, Kuck KH, Ouyang F. Electrophysiological and electrocardiographic predictors of ventricular arrhythmias originating from the left ventricular outflow tract within and below the coronary sinus cusps. *Clin Res Cardiol*. 2015;104:544–554. doi: 10.1007/s00392-015-0817-4
22. Kumagai K. Idiopathic ventricular arrhythmias arising from the left ventricular outflow tract: Tips and tricks. *J Arrhythmia*. 2014;30:211–21.
23. Park KM, Kim YH, Marchlinski FE. Using the surface electrocardiogram to localize the origin of idiopathic ventricular tachycardia. *Pacing Clin Electrophysiol*. 2012;35:1516–1527. doi: 10.1111/j.1540-8159.2012.03488.x
24. Hayashi T, Santangeli P, Pathak RK, Muser D, Liang JJ, Castro SA, Garcia FC, Hutchinson MD, Supple GE, Frankel DS, Riley MP, Lin D, Schaller RD, Dixit S, Callans DJ, Zado ES, Marchlinski FE. Outcomes of catheter ablation of idiopathic outflow tract ventricular arrhythmias with an R wave pattern break in lead V2: a distinct clinical entity. *J Cardiovasc Electrophysiol*. 2017;28:504–514. doi: 10.1111/jce.13183
25. Nagashima K, Choi EK, Lin KY, Kumar S, Tedrow UB, Koplan BA, Michaud GF, John RM, Epstein LM, Tokuda M, Inada K, Couper GS, Stevenson WG. Ventricular arrhythmias near the distal great cardiac vein: challenging arrhythmia for ablation. *Circ Arrhythm Electrophysiol*. 2014;7:906–912. doi: 10.1161/CIRCEP.114.001615
26. Li A, Zuberi Z, Bradfield J, Zarif J, Ward D, Anderson R, Sivkumar K, Saba M. Endocardial ablation of ventricular ectopic beats arising from the basal infero-septal process of the left ventricle. *Heart Rhythm*. 2018;15: 1356–1362.
27. Santangeli P, Hutchinson MD, Supple GE, Callans DJ, Marchlinski FE, Garcia FC. Right Atrial Approach for Ablation of Ventricular Arrhythmias Arising From the Left Posterior-Superior Process of the Left Ventricle. *Circ Arrhythm Electrophysiol*. 2016;9:e004048.
28. Anderson RH, Mohun TJ, Sánchez-Quintana D, Mori S, Spicer DE, Cheung JW, Lerman BB. The anatomic substrates for outflow tract arrhythmias. *Heart Rhythm*. 2018;18:290–297.
29. Liao Z, Zhan X, Wu S, Xue Y, Fang X, Liao H, Deng H, Liang Y, Wei W, Liu Y, Ouyang F. Idiopathic ventricular arrhythmias originating from the pulmonary sinus cusp: prevalence, electrocardiographic/electrophysiological characteristics, and catheter ablation. *J Am Coll Cardiol*. 2015;66: 2633–2644. doi: 10.1016/j.jacc.2015.09.094
30. Dong X, Tang M, Sun Q, Zhang S. Anatomical relevance of ablation to the pulmonary artery root: clinical implications for characterizing the pulmonary sinus of Valsalva and coronary artery. *J Cardiovasc Electrophysiol*. 2018;29:1230–1237.
31. Benhayon D, Nof E, Chik WW, Marchlinski F. Catheter ablation in the right ventricular outflow tract associated with occlusion of left anterior descending coronary artery. *J Cardiovasc Electrophysiol*. 2017;28:347–350. doi: 10.1111/jce.13130
32. Hutchinson MD, Garcia FC. An organized approach to the localization, mapping, and ablation of outflow tract ventricular arrhythmias. *J Cardiovasc Electrophysiol*. 2013;24:1189–1197. doi: 10.1111/jce.12237
33. Ouyang F, Mathew S, Wu S, Kamioka M, Metzner A, Xue Y, Ju W, Yang B, Zhan X, Rillig A, Lin T, Rausch P, Deiß S, Lemes C, Tönnis T, Wissner E, Tilz RR, Kuck KH, Chen M. Ventricular arrhythmias arising from the left ventricular outflow tract below the aortic sinus cusps: mapping and catheter ablation via transseptal approach and electrocardiographic characteristics. *Circ Arrhythm Electrophysiol*. 2014;7:445–455. doi: 10.1161/CIRCEP.114.001690
34. Hai JJ, Chahal AA, Friedman PA, Vaidya VR, Syed FF, DeSimone CV, Nanda S, Brady PA, Madhavan M, Cha YM, McLeod CJ, Mulpuru S, Munger TM, Packer DL, Asirvatham SJ. Electrophysiologic characteristics of ventricular arrhythmias arising from the aortic mitral continuity-potential role of the conduction system. *J Cardiovasc Electrophysiol*. 2015;26:158–163. doi: 10.1111/jce.12587
35. Yamada T, McElderry HT, Doppalapudi H, Okada T, Murakami Y, Yoshida Y, Yoshida N, Inden Y, Murohara T, Plumb VJ, Kay GN. Idiopathic ventricular arrhythmias originating from the left ventricular summit: anatomic concepts relevant to ablation. *Circ Arrhythm Electrophysiol*. 2010;3:616–623. doi: 10.1161/CIRCEP.110.939744
36. Santangeli P, Marchlinski FE, Zado ES, Benhayon D, Hutchinson MD, Lin D, Frankel DS, Riley MP, Supple GE, Garcia FC, Bala R, Desjardins B, Callans DJ, Dixit S. Percutaneous epicardial ablation of ventricular arrhythmias arising from the left ventricular summit: outcomes and electrocardiogram correlates of success. *Circ Arrhythm Electrophysiol*. 2015;8:337–343. doi: 10.1161/CIRCEP.114.002377
37. Baman TS, Ilg KJ, Gupta SK, Good E, Chugh A, Jongnarangsin K, Pelosi F Jr, Ebinger M, Crawford T, Oral H, Morady F, Bogun F. Mapping and ablation of epicardial idiopathic ventricular arrhythmias from within the coronary venous system. *Circ Arrhythm Electrophysiol*. 2010;3:274–279. doi: 10.1161/CIRCEP.109.910802
38. Yang Y, Saenz LC, Varosy PD, Badhwar N, Tan JH, Kilicaslan F, Keung EC, Natale A, Marrouche NF, Scheinman MM. Using the initial vector from surface electrocardiogram to distinguish the site of outflow tract tachycardia. *Pacing Clin Electrophysiol*. 2007;30:891–898. doi: 10.1111/j.1540-8159.2007.00777.x
39. Cheng Z, Cheng K, Deng H, Chen T, Gao P, Zhu K, Fang Q. The R-wave deflection interval in lead V3 combining with R-wave amplitude index in lead V1: a new surface ECG algorithm for distinguishing left from right ventricular outflow tract tachycardia origin in patients with transitional lead at V3. *Int J Cardiol*. 2013;168:1342–1348. doi: 10.1016/j.ijcard.2012.12.013
40. Ito S, Tada H, Naito S, Kurosaki K, Ueda M, Hoshizaki H, Miyamori I, Oshima S, Taniguchi K, Nogami A. Development and validation of an ECG algorithm for identifying the optimal ablation site for idiopathic ventricular outflow tract tachycardia. *J Cardiovasc Electrophysiol*. 2003;14: 1280–1286.
41. Betensky BP, Park RE, Marchlinski FE, Hutchinson MD, Garcia FC, Dixit S, Callans DJ, Cooper JM, Bala R, Lin D, Riley MP, Gerstenfeld EP. The V(2) transition ratio: a new electrocardiographic criterion for distinguishing left from right ventricular outflow tract tachycardia origin. *J Am Coll Cardiol*. 2011;57:2255–2262. doi: 10.1016/j.jacc.2011.01.035
42. Yoshida N, Inden Y, Uchikawa T, Kamiya H, Kitamura K, Shimano M, Tsuji Y, Hirai M, Murohara T. Novel transitional zone index allows more accurate differentiation between idiopathic right ventricular outflow tract and aortic sinus cusp ventricular arrhythmias. *Heart Rhythm*. 2011;8:349–356. doi: 10.1016/j.hrthm.2010.11.023
43. Yoshida N, Yamada T, McElderry HT, Inden Y, Shimano M, Murohara T, Kumar V, Doppalapudi H, Plumb VJ, Kay GN. A novel electrocardiographic criterion for differentiating a left from right ventricular outflow tract tachycardia origin: the V2S/V3R index. *J Cardiovasc Electrophysiol*. 2014;25:747–753. doi: 10.1111/jce.12392
44. He Z, Liu M, Yu M, Lu N, Li J, Xu T, Zhu J, O'Gara MC, O'Meara M, Ye H, Tan X. An electrocardiographic diagnostic model for differentiating left from right ventricular outflow tract tachycardia origin. *J Cardiovasc Electrophysiol*. 2018;29:908–915.
45. Kaypakli O, Koca H, Sahin DY, Karataş F, Ozbicer S, Koç M. S-R difference in V1-V2 is a novel criterion for differentiating the left from right ventricular outflow tract arrhythmias. *Ann Noninvasive Electrocardiol*. 2018;23:e12516. doi: 10.1111/anec.12516
46. Zhang F, Chen M, Yang B, Ju W, Chen H, Yu J, Lau CP, Cao K, Tse HF. Electrocardiographic algorithm to identify the optimal target ablation site for idiopathic right ventricular outflow tract ventricular premature contraction. *Europace*. 2009;11:1214–1220. doi: 10.1093/europace/eup231
47. Tada H, Ito S, Naito S, Kurosaki K, Kubota S, Sugiyasu A, Tsuchiya T, Miyaji K, Yamada M, Kutsumi Y, Oshima S, Nogami A, Taniguchi K. Idiopathic ventricular arrhythmia arising from the mitral annulus: a distinct subgroup of idiopathic ventricular arrhythmias. *J Am Coll Cardiol*. 2005;45:877–886. doi: 10.1016/j.jacc.2004.12.025
48. Kumagai K, Yamauchi Y, Takahashi A, Yokoyama Y, Sekiguchi Y, Watanabe J, Iesaka Y, Shirato K, Aonuma K. Idiopathic left ventricular tachycardia originating from the mitral annulus. *J Cardiovasc Electrophysiol*. 2005;16:1029–1036. doi: 10.1111/j.1540-8167.2005.40749.x
49. Herczku C, Berruezo A, Andreu D, Fernández-Armenta J, Mont L, Borràs R, Arbelo E, Tolosana JM, Trucco E, Ríos J, Brugada J. Mapping data predictors of a left ventricular outflow tract origin of idiopathic ventricular

Downloaded from http://ahajournals.org by on May 28, 2022

tachycardia with V3 transition and septal earliest activation. *Circ Arrhythm Electrophysiol*. 2012;5:484–491. doi: 10.1161/CIRCEP.111.969592
50. Yamada S, Chung FP, Lin YJ, Chang SL, Lo LW, Hu YF, Tuan TC, Chao TF, Liao JN, Lin CH, Lin CY, Chang YT, Chang TY, Te ALD, Chen SA. Electrocardiographic features of failed and recurrent right ventricular outflow tract catheter ablation of idiopathic ventricular arrhythmias. *J Cardiovasc Electrophysiol*. 2018;29:127–137. doi: 10.1111/jce.13359
51. Nakano M, Ueda M, Ishimura M, Kajiyama T, Hashiguchi N, Kanaeda T, Kondo Y, Hiranuma Y, Kobayashi Y. Estimation of the origin of ventricular outflow tract arrhythmia using synthesized right-sided chest leads. *Europace*. 2014;16:1373–1378. doi: 10.1093/europace/eut355
52. Igarashi M, Nogami A, Sekiguchi Y, Kuroki K, Yamasaki H, Machino T, Yui Y, Ogawa K, Talib AK, Murakoshi N, Kuga K, Aonuma K. The QRS morphology pattern in V5R is a novel and simple parameter for differentiating the origin of idiopathic outflow tract ventricular arrhythmias. *Europace*. 2015;17:1107–1116. doi: 10.1093/europace/euu337
53. Miyamoto K, Yokokawa M, Tanaka K, Nagai T, Okamura H, Noda T, Satomi K, Suyama K, Kurita T, Aihara N, Kamakura S, Shimizu W. Diagnostic and prognostic value of a type 1 Brugada electrocardiogram at higher (third or second) V1 to V2 recording in men with Brugada syndrome. *Am J Cardiol*. 2007;99:53–57. doi: 10.1016/j.amjcard.2006.07.062
54. Anter E, Frankel DS, Marchlinski FE, Dixit S. Effect of electrocardiographic lead placement on localization of outflow tract tachycardias. *Heart Rhythm*. 2012;9:697–703. doi: 10.1016/j.hrthm.2011.12.007
55. Zhang F, Hamon D, Fang Z, Xu Y, Yang B, Ju W, Bradfield J, Shivkumar K, Chen M, Tung R. Value of a posterior electrocardiographic lead for localization of ventricular outflow tract arrhythmias: the V4/V8 ratio. *JACC Clin Electrophysiol*. 2017;3:678–686. doi: 10.1016/j.jacep.2016.12.018
56. Cheng D, Ju W, Zhu L, Chen K, Zhang F, Chen H, Yang G, Li X, Li M, Gu K, Han B, Fan J, Lin Y, Cao K, Kojodjojo P, Yang B, Chen M. V3 R/V7 index a novel electrocardiographic criterion for differentiating left from right ventricular outflow tract arrhythmias origins. *Circ Arrhythm Electrophysiol*. 2018;11:e006243. doi: 10.1161/CIRCEP.118.006243
57. Lee A, Denman R, Haqqani HM. Ventricular ectopy in the context of left ventricular systolic dysfunction: risk factors and outcomes following catheter ablation. *Heart Lung Circ*. 2018;28:379–388.
58. Bradfield JS, Homsi M, Shivkumar K, Miller JM. Coupling interval variability differentiates ventricular ectopic complexes arising in the aortic sinus of Valsalva and great cardiac vein from other sources: mechanistic and arrhythmic risk implications. *J Am Coll Cardiol*. 2014;63:2151–2158. doi: 10.1016/j.jacc.2014.02.551
59. Bogun F, Taj M, Ting M, Kim HM, Reich S, Good E, Jongnarangsin K, Chugh A, Pelosi F, Oral H, Morady F. Spatial resolution of pace mapping of idiopathic ventricular tachycardia/ectopy originating in the right ventricular outflow tract. *Heart Rhythm*. 2008;5:339–344. doi: 10.1016/j.hrthm.2007.11.011
60. Azegami K, Wilber DJ, Arruda M, Lin AC, Denman RA. Spatial resolution of pacemapping and activation mapping in patients with idiopathic right ventricular outflow tract tachycardia. *J Cardiovasc Electrophysiol*. 2005;16:823–829. doi: 10.1111/j.1540-8167.2005.50041.x
61. Selcuk MT, Balci KG, Maden O, Selcuk H, Vicdan M, Kalender E, Balci MM. Comparison of the predictive accuracy of four different ECG algorithms in identification of true ablation site for the idiopathic right ventricular outflow tract tachycardias. *Ann Noninvasive Electrocardiol*. 2018;23:e12529. doi: 10.1111/anec.12529
62. Yamada T, Murakami Y, Yoshida N, Okada T, Shimizu T, Toyama J, zYoshida Y, Tsuboi N, Muto M, Inden Y, Hirai M, Murohara T, McElderry HT, Epstein AE, Plumb VJ, Kay GN. Preferential conduction across the ventricular outflow septum in ventricular arrhythmias originating from the aortic sinus cusp. *J Am Coll Cardiol*. 2007;50:884–891. doi: 10.1016/j.jacc.2007.05.021
63. Shirai Y, Liang JJ, Garcia FC, Supple GE, Callans DJ, Zado ES, Marchlinski FE, Santangeli P. QRS morphology shift following catheter ablation of idiopathic outflow tract ventricular arrhythmias: Prevalence, mapping features, and ablation outcomes. *J Cardiovasc Electrophysiol*. 2018;29:1664–1671. doi: 10.1111/jce.13728

Downloaded from http://ahajournals.org by on May 28, 2022